

Effects of alloying elements on the phase constitution and microstructure of *in situ* SiC/Al composites

Hongyu Yang*, Erting Dong[†], Bingqi Zhang[‡], Liangyu Chen[§],
Yunxue Jin* and Shili Shu^{*,¶,||}

*School of Materials Science and Engineering,
Jiangsu University of Science and Technology,
Zhenjiang 212003, Jiangsu, P. R. China

[†]Department of Materials Engineering, Henan Institute of Technology,
Xinxiang 453000, P. R. China

[‡]Datang Northeast Electric Power Test and Research Institute,
No. 3195 Weishan Street, Changchun 130000, P. R. China

[§]School of Science, Jiangsu University of Science and Technology,
Zhenjiang 212003, P. R. China

[¶]State Key Laboratory of Luminescence and Applications,
Changchun Institute of Optics,
Fine Mechanics and Physics, Chinese Academy of Sciences,
Changchun 130033, P. R. China

^{||}shushili@ciomp.ac.cn

Received 1 July 2018

Revised 30 August 2018

Accepted 15 September 2018

Published 11 January 2019

In this work, the *in situ* SiC/Al composites were successfully fabricated by the method of combustion synthesis and hot press consolidation in an Al-C-Si system. The effect of alloying elements (Mn, Zn, Ti) on the phase constitution and microstructure of *in situ* SiC/Al composites were investigated. Results indicated that the $Al_{11}Mn_{14}$ and Ti_xSi_y phases were formed in the SiC/Al composites with the addition of Mn and Ti, respectively. By the addition of Mn, the size of the synthesized SiC particles was obviously reduced, and consequently the amount of SiC particles was increased. Meanwhile, the percentage of the submicro SiC particles increased about from 22% to 83%. However, the addition of Zn and Ti had little effect on the size of SiC particles.

Keywords: *In situ* SiC/Al composites; alloying elements; combustion synthesis.

PACS numbers: 81.05.Mh, 81.05.Bx

^{||}Corresponding author.

1. Introduction

Aluminum is widely applied in industry because it possesses superior ductility and light weight.¹ However, the application of aluminum is hindered by its low wear resistance properties and poor elevated temperature stability. To improve the mechanical properties of Al metal, the hard and fine ceramic particles need to be uniformly dispersed into the Al matrix.² The SiC ceramic particles own outstanding properties such as high stiffness and hardness, good thermal stability and low thermal coefficient of expansion. They were proposed to be added into the Al matrix to form the SiC/Al composites.³ Most reports⁴ showed that the reinforcing SiC particles were directly added into the Al matrix to form *ex situ* SiC/Al composites. Nevertheless, in such SiC/Al composites, the interface bonding between SiC and Al matrix is weak and cracks are easy to appear due to the contamination and existence of thin oxide layers on the surface of the *ex situ* SiC particles.⁵ In addition, the reinforcing SiC particles are difficult to uniformly disperse into the Al matrix.⁶ Compared to the *ex situ* methods, in the *in situ* fabricating methods, in the reinforcing particles are synthesized via chemical reactions among the pristine elemental materials themselves. It can form the stable reinforcement in the matrix and the clean interfaces with high bonding strength between reinforcement and matrix were formed.⁷ Meanwhile, the size of the synthesized reinforcing particles is fine and the particles could uniformly distribute in the matrix.⁸ However, the *in situ* SiC particles are difficult to be directly synthesized in Al melts, which is due to the limited solubility of carbon in Al-Si melts.⁹ Nie *et al.*¹⁰ fabricated the *in situ* SiC/Al composites by the structural evolution of TiC in Al-Si melt. They reported that the synthesis of SiC particles occurred via the gradual reaction between TiC and Si atoms, and the simultaneously formed needle-like TiAl_xSi_y phase would play a detrimental role in the mechanical properties of the composites. Du and Gao *et al.*¹¹ reported that the *in situ* synthesized SiC particles through gradual phase transformation mechanism were feasible. They fabricated the *in situ* SiC/Al composites by the master alloy casting method.¹² While, to our knowledge, the method of combustion synthesis combined with pressure consolidation is also an effective way for the *in situ* synthesized metal matrix composites.^{13,14} This method can form the dense and high purity composite with one-step process and low energy requirement.

As we know, the phase constitution and size of SiC particles in SiC/Al composites plays a significant role in determining the comprehensive properties and actual application for SiC/Al composites.¹⁵ While, for *in situ* synthesized ceramic particle reinforced metal matrix composites, alloying element is a key factor in affecting the phase constitution and ceramic particle size of the composites. Therefore, further researches on the effect of different alloying elements on the phase constitution and microstructure of the *in situ* synthesized SiC/Al composites are essential. Thus, in this work, we fabricated *in situ* SiC/Al composites by the method of combustion synthesis and hot press consolidation in an Al-Si-C system. Moreover, the effect of

alloying elements (Mn, Zn and Ti) on phase constitution and microstructure of the *in situ* synthesized SiC/Al composites was investigated.

2. Experimental

The commercial Al powders (99.7 wt.% purity, $\sim 48 \mu\text{m}$), Si powders (99.9 wt.% purity, $\sim 48 \mu\text{m}$), C-black powders (99.9 wt.% purity, $\sim 0.1 \mu\text{m}$), and powders of alloying elements (Mn, Zn and Ti, 99.5 wt.% purity, $\sim 48 \mu\text{m}$) were used for powder blends. The above raw metal and alloy powders are provided by Shanghai st-nano science and technology Co., Ltd. The starting composition of the green samples was Al-20Si-5C (wt.%) and Al-20Si-5C-3Me (wt.%, Me = Mn, Zn, Ti, respectively). First, the raw powders were sufficiently mixed in a stainless steel die by ball milling for 8 h with low speed ($\sim 35 \text{ rpm}$). Second, the mixtures were cold pressed into cylindrical compacts with the diameter of 28 mm and height of 30 mm. Third, the powder compact was contained in a graphite mold. The graphite mold with powder compact was put in a self-made vacuum thermal explosion furnace. Then, the combustion synthesis and hot press consolidation experiment were conducted. During the process, the compact was heated at the speed of $20^\circ\text{C}/\text{min}$ in a vacuum atmosphere, the temperature was controlled by W5-Re26 thermocouples. When the temperature reached the goal value, the compact was hot pressed with 30 MPa for 15 min and then the sample was cooled down to ambient temperature.

The phase constitution of the samples was investigated by X-ray diffraction (XRD, Model D/Max 2500PC, Rigaku, Tokyo, Japan) with $\text{Cu K}\alpha$ ($\lambda = 0.154 \text{ nm}$) radiation. The morphology was observed by scanning electron microscopy (SEM, Model Evo18 Carl Zeiss, Oberkochen, Germany). The size measurement and distribution statistics of SiC particles were performed with the Nano Measurer software.

3. Results and Discussion

3.1. Formation of *in situ* SiC/Al composites in the Al-20Si-5C system

The sinter temperature is a thermodynamic factor of synthesis SiC. In order to investigate the effects of sintering temperature on the synthesis reaction and determine the suitable sintering temperature, we fabricated the SiC/Al composites at the temperature of 750°C , 850°C and 950°C , respectively.

Figure 1 shows the XRD patterns of the Al-20Si-5C samples fabricated at different sintering temperatures. It can be seen from Fig. 1(a) that there are no diffraction peaks corresponding to the SiC phase. However, the Al_4C_3 phase is detected in the composite fabricated at 750°C . When the sintering temperature increases to 850°C , it can be seen that both Al_4C_3 phase and SiC phase are presented, as shown in Fig. 1(b). When the sintering temperature increases up to 950°C , the Al_4C_3 phase disappears and the diffraction peak intensity of SiC phase increases, as shown in Fig. 1(c).

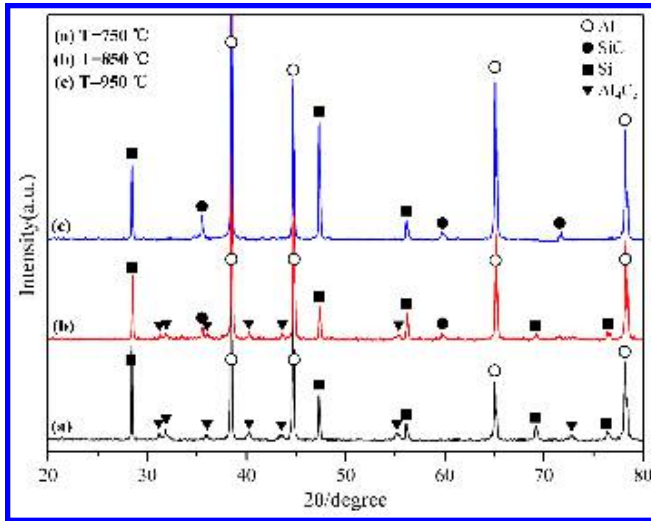


Fig. 1. (Color online) The XRD patterns of the sample fabricated at different sintering temperatures.

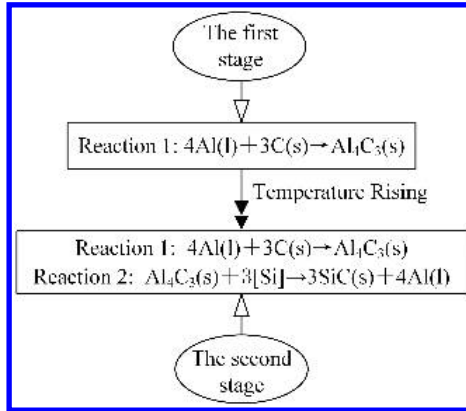


Fig. 2. The *in situ* reaction process of SiC/Al composites.

The XRD results indicate that the Al_4C_3 phase forms firstly during the preparation of the SiC/Al composites. Then the Al_4C_3 as the transition phase provides carbon source which reacts with Si to generate SiC.¹¹ Therefore, the *in situ* synthetic reaction process of SiC particle by the method of combustion synthesis and hot press consolidation is presented, as shown in Fig. 2.

When the sintering temperature is 750°C, based on the thermodynamic data listed in Table 1, the formation energy of Al_4C_3 is about -180.79 kJ/mol, while the formation energy of SiC is -65.09 kJ/mol, which illustrates the formation of Al_4C_3 is more favorable in the low-temperature aluminum melt. The Gibbs free

Table 1. The thermodynamic Gibbs free energy change in the Al-Si-C system.¹⁶

Reaction	ΔG^0 , J/mol (T , K)
Si(s) \rightarrow Si(l)	$\Delta G^0 = 50540 - 30.0T$ ($298\text{K} < T < 1680\text{K}$)
Si(s) + C(s) \rightarrow SiC(s)	$\Delta G^0 = -73220 + 7.95T$
C(s) + 4/3Al(l) \rightarrow 1/3Al ₄ C ₃ (s)	$\Delta G^0 = -69092 + 8.63T$
i(l) \rightarrow [i]	$\Delta G^0 = -RT \ln(100M_i/\gamma_i^h M_i)$

energy change of reaction 2 is as follows:

$$\Delta G^0 = 3\Delta G_{\text{SiC}} + 4RT \ln a_{[\text{Al}]} - \Delta G_{\text{Al}_4\text{C}_3} - 3RT \ln a_{[\text{Si}]}, \quad (1)$$

where the ΔG_{SiC} and $\Delta G_{\text{Al}_4\text{C}_3}$ are the Gibbs formation energy of SiC and Al₄C₃, respectively. The $a_{[\text{Al}]}$ and $a_{[\text{Si}]}$ are the activities of [Al] and [Si] in the Al-Si binary system, respectively. On the basis of the Wilson equation and an extended Miedema model,¹² the G^0 can be expressed as

$$\Delta G^0 = 3\Delta G_{\text{SiC}} - \Delta G_{\text{Al}_4\text{C}_3} + RT \ln \frac{(\chi_{\text{Al}} \cdot \gamma_{\text{Al}})^4}{(\chi_{\text{Si}} \cdot \gamma_{\text{Si}})^3}, \quad (2)$$

where χ_i is the mole fraction in aluminum melt, γ_i is the activity coefficient. When the sintering temperature increases to 850°C, the ΔG^0 is calculated to be about -28.019 kJ/mol, indicating that the reaction 2 can take place spontaneously at 850°C. However, the Al₄C₃ phase can still be detected at this moment [Fig. 1(b)]. Until the sintering temperature increases to 950°C, the generated Al₄C₃ phases are completely consumed. The reason is that the system energy increases with the increase of sintering temperature, which is in favor of the diffusion of Si atoms in the aluminum melt.

Figure 3 shows the SEM images and EDS result of the etched surfaces of Al-20Si-5C sample fabricated at the sintering temperature of 950°C. It can be seen that a large quantity of irregular blocky-shaped particles is distributed in the Al

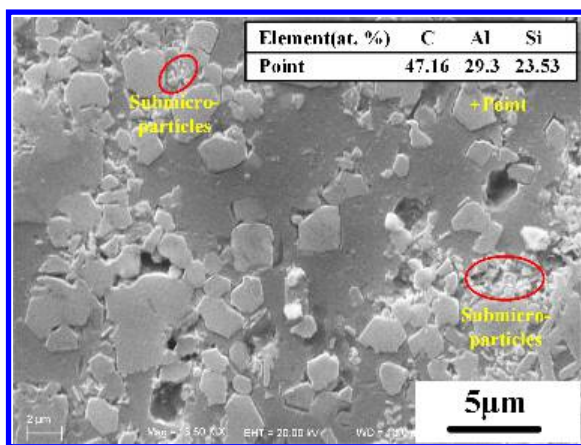


Fig. 3. (Color online) The SEM images of the sample fabricated at 950°C and EDS analysis.

matrix and there are some submicro-particles in the vicinity of the irregular blocky-shaped particles. These particles are identified as SiC by EDS analysis, which can be confirmed by the element contents of Si and C. These above results indicate that the SiC/Al composites can be *in situ* synthesized at the sintering temperature of 950°C by combustion synthesis and hot press consolidation.

3.2. Effects of alloying elements

In order to investigate the effect of alloying element addition on the SiC/Al composites, 3 wt.% Mn, 3 wt.% Zn and 3 wt.% Ti were added into the Al-20Si-5C system, respectively. Then the *in situ* synthesized experiments were performed at the sintering temperature of 950°C.

Figure 4 shows the XRD patterns of the SiC/Al composites with the additions of Mn, Zn and Ti. The products in these samples all contain SiC phase. In addition, the $Al_{11}Mn_{14}$ and Ti_xSi_y are identified in the Al-20Si-5C-3Mn and Al-20Si-5C-3Ti samples, respectively, as show in Figs. 4(a) and 4(c). Besides, there are no zinc compounds or Zn are detected in the Al-20Si-5C-3Zn system, as shown in Fig. 4(b). This could be attributed to the evaporation of the Zn during the heating and combustion processes.¹⁷

Figure 5 shows the SEM images of the etched surfaces of the SiC/Al composites with the additions of Mn, Zn and Ti. It clearly reveals the irregular blocky-shaped SiC particles in these samples, indicating that these alloying elements cannot affect the morphology of SiC particle. Nevertheless, compared to Figs. 3(a) and 5, it is obvious to find that the size of SiC particles decreases in different degrees with the addition of different alloying elements.

Figure 6 shows the corresponding size distribution histograms of the SiC particles in the fabricated *in situ* SiC/Al composites with different alloying element addition. As shown in Fig. 6(a), the maximum size and average size of SiC particles in the SiC/Al composite without alloying element addition are about 4.1

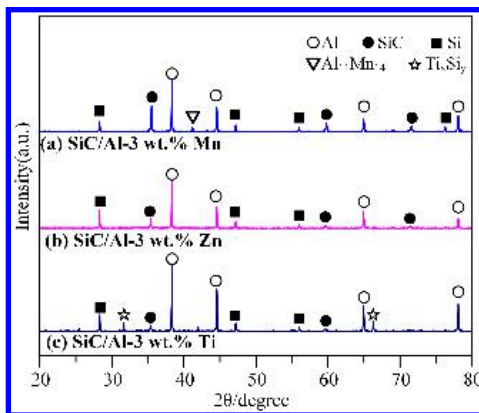


Fig. 4. (Color online) The XRD patterns of the SiC/Al composites with the alloying element.

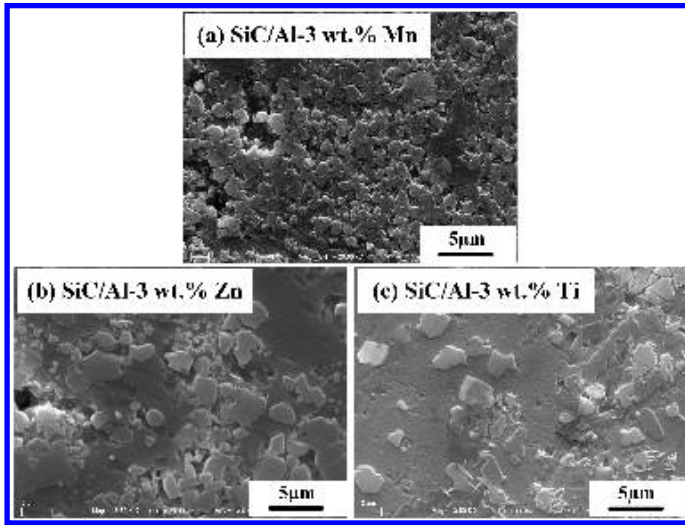


Fig. 5. SEM images of the etched surfaces of the SiC/Al composites with the alloying element.

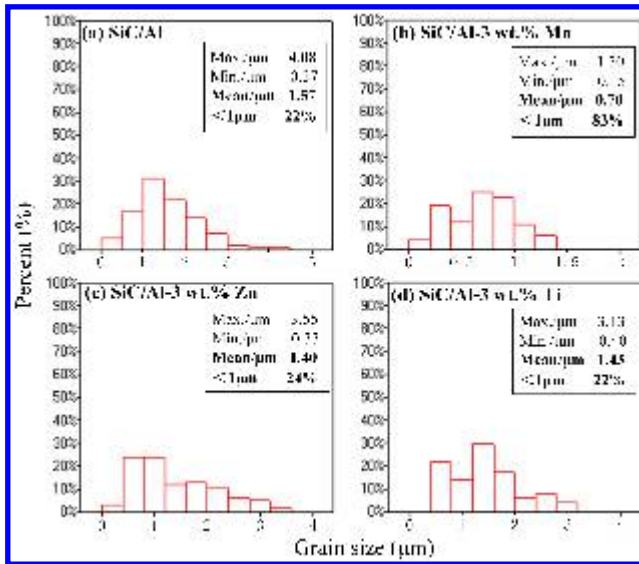


Fig. 6. (Color online) Size distribution of the SiC particles in these composites.

and 1.6 μm , respectively. In addition, the percentage of the SiC particles in sub-micro size is about 22% in total. As shown in Fig. 6(b), by addition of 3 wt.% Mn, the maximum size and average size of SiC particle are reduced to 1.3 and 0.7 μm , and the size of some SiC particles can even reach to less than 0.2 μm . Meanwhile, the percentage of submicro-particle increases to about 83%. That means the addition of Mn element can significantly reduce the size of SiC particles and lead to

more uniform distribution of the particle size. As shown in Figs. 6(c) and 6(d), by addition of Zn and Ti, the maximum size of SiC particle reduces to 3.6 and 3.1 μm , respectively. The addition of Zn and Ti has a little influence on the size of SiC particle relative to the addition of Mn.

The reason for the size refinement of SiC particles by addition of Mn should be that Mn addition can decrease the solidus temperature of the Al-Si-C system.¹⁸ The lower solidus temperature results in the formation of liquid phase at lower temperature. These contribute to the decrease of the synthesis temperature of SiC particles, leading to high degree of supercooling and increase of SiC nucleation rate. Thus, the amount of SiC particle increases and consequently the size of SiC particle decreases. According to the report,¹⁹ the strength of aluminum matrix composites can be improved by approximately 20% when the reinforcement particle size is decreased from a micrometer to a sub-micrometer. Therefore, it is reasonable to believe that the addition of Mn element is beneficial to the *in situ* SiC/Al composites.

4. Conclusions

In this work, the *in situ* SiC/Al composites were successfully fabricated by the method of combustion synthesis and hot press consolidation. The $\text{Al}_{11}\text{Mn}_{14}$ and Ti_xSi_y phases were formed in the SiC/Al composites with the addition of Mn and Ti, respectively. The addition of Mn leads to a more uniform distribution of the SiC particle size. Meanwhile, it reduces the maximum size and average size of SiC particles from 4.1 and 1.6 μm to 1.3 and 0.7 μm , respectively. Besides, by addition of Mn, the percentage of submicro SiC particles increases from 22% to 83%. However, the addition of Zn and Ti had little effect on the size of SiC particles.

Acknowledgment

This work is supported by the National Natural Science Foundation of China (NNSFC, Nos. 51701086 and 51501176).

References

1. N. Gangil, A. N. Siddiquee and S. Maheshwari, *J. Alloy. Compd.* **715**, 91 (2017).
2. D. Yang et al., *Mater. Des.* **87**, 1100 (2015).
3. L. J. Zhang et al., *Mater. Sci. Eng. A* **626**, 338 (2015).
4. H. Lee et al., *Mater. Sci. Eng. A* **680**, 368 (2017).
5. L. Wang et al., *Mater.* **8**, 8839 (2015).
6. I. A. Ibrahim, F. A. Mohamed and E. J. Lavernia, *J. Mater. Sci.* **26**, 1137 (1991).
7. B. Almangour, D. Grzesiak and J. M. Yang, *J. Alloy. Compd.* **706**, 409 (2017).
8. S. C. Tjong and Z. Y. Ma, *Mater. Sci. Eng. R* **29**, 49 (2000).
9. L. L. Oden and R. A. Mccune, *Metall. Mater. Trans. A* **18**, 2005 (1987).
10. J. Nie et al., *J. Alloy. Compd.* **613**, 407 (2014).
11. X. Du et al., *J. Alloy. Compd.* **588**, 374 (2014).
12. T. Gao et al., *J. Alloy. Compd.* **685**, 91 (2016).
13. L. Wang et al., *Mater. Charact.* **125**, 7 (2017).

14. L. Wang *et al.*, *Sci. Rep.* **7**, 4540 (2017).
15. S. Kumar and V. Balasubramanian, *Tribol. Int.* **43**, 414 (2010).
16. G. M. Wilson, *J. Am. Chem. Soc.* **86**, 127 (1964).
17. H. Y. Wang *et al.*, *J. Mater. Sci.* **40**, 1255 (2005).
18. X. Du *et al.*, *Mater. Des.* **63**, 194 (2014).
19. B. Dikici and M. Gavgali, *J. Alloy. Compd.* **551**, 101 (2013).